NASA Contractor Report 194934

ICASE Report No. 94-48

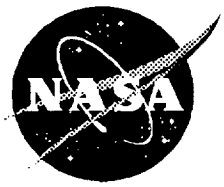

ICASE

ON THE INTERACTION OF JET NOISE WITH A NEARBY FLEXIBLE STRUCTURE

J. L. McGreevy
A. Bayliss
L. Maestrello

Contract NAS1-19480
June 1994

Institute for Computer Applications in Science and Engineering
NASA Langley Research Center
Hampton, VA 23681-0001

Operated by Universities Space Research Association

ICASE Fluid Mechanics

Due to increasing research being conducted at ICASE in the field of fluid mechanics, future ICASE reports in this area of research will be printed with a green cover. Applied and numerical mathematics reports will have the familiar blue cover, while computer science reports will have yellow covers. In all other aspects the reports will remain the same; in particular, they will continue to be submitted to the appropriate journals or conferences for formal publication.

ON THE INTERACTION OF JET NOISE WITH A NEARBY FLEXIBLE STRUCTURE

J. L. McGreevy, A. Bayliss*, L. Maestrello
NASA Langley Research Center
Hampton, VA 23681-0001

Abstract

The model of the interaction of the noise from a spreading subsonic jet with a panel-stringer assembly is studied numerically in two dimensions. The radiation resulting from this flow/acoustic/structure coupling is computed and analyzed in both the time and frequency domains. The jet is initially excited by a pulse-like source inserted into the flow field. The pulse triggers instabilities associated with the inviscid instability of the jet mean flow shear layer. These instabilities in turn generate sound which provides the primary loading for the panels. The resulting structural vibration and radiation depends strongly on their placement relative to the jet/nozzle configuration. Results are obtained for the panel responses as well as the transmitted and incident pressure. The effect of the panels is to act as a narrow filter, converting the relatively broad band forcing, heavily influenced by jet instabilities, into radiation concentrated in narrow spectral bands.

*Dept. of Engineering Sciences and Applied Mathematics, Northwestern University, Evanston, IL. Partially supported by NASA Langley Research Center under contract NAS1-19480 while in residence at ICASE.

1. Introduction

In this paper we study numerically the interaction between jet noise, emanating from a high subsonic jet, with a flexible aircraft-type structure. The emphasis is on (1) jet noise generated by spatially growing instabilities associated with the shear layer of the jet as an excitation mechanism for the flexible structure, (2) the resulting vibration of and radiation from the flexible structure due to the flow/acoustic/structure coupling and (3) the effect of the placement of the panels, relative to the jet/nozzle configuration, on panel response and radiation. The precise details of the jet flow field are deemphasized via the use of a model jet flow field in the Euler equations.

The numerical computations presented here are a step in determining the role of jet noise excitation on both structural fatigue (sonic fatigue) of aircraft panel assemblies and interior aircraft noise levels. The results demonstrate the important role of instability wave generated sound on the frequency response of and radiation from the ensuing structural vibration. In particular, since instability wave generated sound is highly directional, the panel placement relative to the jet/nozzle configuration is an important factor in determining the resulting panel response.

The jet is excited by a pulse starter, an artificially imposed source that triggers continuous perturbations in the flow field. We concentrate on the long time behavior of the excited jet, i.e. the behavior of unsteady disturbances in the jet long after the initial disturbance generated by the pulse has propagated from the region of interest. The pulse starter is applied to the Euler equations, suitably modified so that only disturbances in a realistic spreading jet profile are computed. As a result of the pulse, an initial acoustic disturbance is generated. This acoustic disturbance propagates into the farfield while undergoing convection and dispersion due to the flow field. More importantly, the initial disturbance triggers the development of an instability wave, i.e., a large scale structure which is slowly convected downstream along the jet axis, due to interaction with the unstable jet shear layer. This instability wave, which is qualitatively similar to structures observed in real jets, is a source of jet noise as it triggers the development of other instability waves in a continuous fashion long after the initial disturbance due to the pulse has propagated away from the flow field and the panels. In particular, the qualitative features of large scale instability waves as sources of jet noise are simulated [7, 16, 22, 34]. The model also allows simulation of dispersive effects such as the frequency dependent refraction of sound by the flow field.

The use of the pulse starter allows the qualitative simulation of instability wave generated sound in a spreading jet, a key component of real jet noise, with sufficiently reduced computational requirements so that high resolution computations of the fully coupled flow/acoustic/structure interaction can be readily obtained. This methodology is similar to that employed in [2, 21, 22] where the behavior of instability wave generated sound in subsonic axisymmetric jets (without any nearby structure) was considered. These results demonstrated that the starter pulse was effective as a computational tool to excite instability wave generated sound and to study the bending (refraction effect) of sound waves through the jet flow field. The results also demonstrated that the instability wave generated sound was highly directional, peaking at low to mid angles from the jet axis, and concentrated at low frequencies.

There have been many important studies on jet noise. The sources of jet noise were recognized in the Lighthill acoustic analogy [17]. The resulting model led to scaling arguments for the dependence of the farfield sound on jet velocity, although the actual sources had to be modeled for calculation purposes. An independent theory of sound radiation, using a different formulation of the sources, was obtained in [29]. Extensions of this work to account for shear interaction terms and vortical

flows followed [18, 28, 33]. Experiments demonstrated the existence of large scale structures or instability waves in jets and the role of instability wave generated sound as an important component of jet noise [7, 16, 22, 34]. Analytical studies provided further elucidation of the role of instabilities as an important source of jet noise [5, 13, 14, 26, 27, 30] as did the computations [2, 21, 22].

More recent computations have included the effect of viscosity and turbulence models, for example, [25]. These computations demonstrated the substantial difficulties in simulating sound generation from spreading jets directly from the Navier-Stokes equations. In the approach taken here, the jet profile is modeled and included as a source term in the Euler equations. The resulting model allows the formation of inviscid instabilities and associated jet noise, which qualitatively models many of the observed features of the natural sources of sound in subsonic jets. The model also allows for the effect of convection and dispersion of acoustic waves due to the flow field.

An understanding of the nature of the jet forcing is an essential prerequisite to an understanding of the role of jet noise on the structural vibration of aircraft panels. Since instability waves are one of the most important sources of jet noise, particularly for subsonic jets, it is important to determine the role of instability wave generated sound as a forcing mechanism for flexible aircraft panels.

For sources that can be well approximated by modes of the panel, simple normal mode analysis suggests that the displacement would exhibit spectral peaks near the resonant frequencies of the panel, i.e., the natural frequencies. Even for such sources, other quantities such as the velocity and the radiated pressure, which must be obtained from solution of the wave equation (either fully coupled to the panel motion as done here or á posteriori using the uncoupled panel velocity as a boundary condition) will not necessarily exhibit spectral peaks at the natural frequencies. The spectrum of these quantities will depend on both the details of the forcing function and on the parameters of the panels. When the incident pressure is jet noise, as considered here, the situation is yet more complicated as the sources will be convecting downstream with the flow and may not be well approximated by modes of the panel. In this case even qualitative details of panel response would be expected to require specification of the sources accounting for the most physically relevant features of jet noise generation.

Various approaches have been employed to determine panel response in a system exhibiting flow/acoustic/structure interaction. The sources can be taken from experimental measurements, (e.g., [8, 24]). Another approach is to model the sources using appropriate simplifications (eg., [6, 35]). In the former case, the panel response could then itself be measured experimentally as in [20] or computed via solution of the resulting panel equation from the measured sources as in [8, 24]. While recent experiments [20] in supersonic jets have succeeded in isolating features of panel response due to oscillating shocks and jet instability, in general the use of experimental measurements dictates that all physical mechanisms associated with the jet noise be intertwined, thus making it difficult to ascertain the role of individual physical mechanisms of jet noise on panel response.

The modeling of sources necessarily involves significant simplifications of an extremely complex phenomena, namely the generation and propagation of jet noise, and also typically does not account for the full fluid/acoustic/structure coupling of the panel response. In the present work, we focus primarily on the role of sound generated from instability waves, large scale structures associated with the inviscid instability of the jet shear layer, as an excitation mechanism for the structural vibration. Such waves are known to be important sources of jet noise for both subsonic and supersonic jets [16]. The computations, while employing a model jet, are able to simulate the

qualitative features of such noise and the ensuing panel response and radiation. We employ a computational model in which the panel response and resulting radiation are fully coupled to the evolution of disturbances in the jet flow field. Similar fully coupled calculations were employed in [9] where the response of a panel to a normally incident plane acoustic wave was considered. The computations simulated many of the features observed experimentally in [23]. The results demonstrated that highly complex responses, including subharmonic formation, quasi-periodic and possibly chaotic responses could be obtained for sufficiently high excitation level.

Our results demonstrate that the forcing due to instability wave generated sound can lead to enhanced low frequency vibration and radiation from the panels. The effectiveness of jet instabilities in exciting the panel is highly dependent on the placement of the panel relative to the jet exit. The panel acts as a narrow filter in converting a relatively broadband forcing field, heavily influenced by jet instabilities, into a relatively discrete vibration and radiation spectrum. The resulting radiation is beamed primarily in the vertical and downstream directions. While the precise frequencies of the radiation will depend on the details of the flow field and the mechanism of exciting the jet shear layer instabilities, we believe that the general features of the panel response presented here illustrate the role of jet noise in exciting vibration and radiation from nearby surfaces.

In section 2 we describe the model and the resulting numerical method. In section 3 we describe our results. In section 4 we summarize our conclusions.

2. Problem Formulation

The computational domain is shown in Figure 1. Fluctuating pressure, density and velocities are computed in two domains, that which contains the jet, exiting from a nozzle of width D, and the domain on the other side of the wall boundary. We will refer to the two domains as the jet and radiation domains respectively. The wall boundary is a rigid wall containing two adjacent flexible cutout sections (denoted A and B in Figure 1) with rigidly clamped boundaries. The panels vibrate in response to excitation from jet noise and radiate sound into both domains. We focus primarily on acoustic radiation into the radiation domain, as the radiation into the jet domain is small compared to the large disturbances already present in the jet.

The numerical method involves coupling the computation of a nonlinear equation governing the panel responses (the beam equation) to an Euler computation performed separately in both the jet and radiation domains. The difference in pressure across the panels (computed from the Euler equations) is the source term for the beam equation, and its solution provides the normal velocity to be used as a boundary equation for the Euler equations. We assume that the panel displacement is small relative to the acoustic wavelengths so that in each of the two Euler computations the normal velocity (obtained from the beam equation) is imposed at $y = 0$.

In the jet domain the Euler equations are modified to account for the jet flow. We assume a straight pipe of width D from which the jet exits. The solution is computed both within and exterior to the pipe, while rigid boundary conditions are assumed on each side. In the radiation domain, the Euler equations are directly computed. We note that for linear radiation, an alternative is to impose the radiation condition as in [32]. Thus, in the computations presented here, the jet flow field is fully coupled to the panel vibration and ensuing radiation.

The nonlinear beam equation is given by

$$D_p \frac{\partial^4 z}{\partial x^4} - N_x \frac{\partial^2 z}{\partial x^2} + \rho_p h \frac{\partial^2 z}{\partial t^2} + \gamma \frac{\partial z}{\partial t} = p^+ - p^-, \tag{1}$$

where z represents the plate transverse deflection, ρ_p the mass per unit volume of the plate, h the plate thickness, γ the physical damping, and $D_p = Mh^3/12(1-\nu^2)$ is the stiffness of the plate where M is the modulus of elasticity and ν is the Poisson ratio of the plate material. The coefficient N_x of the nonlinear term is given by

$$N_x = \frac{Mh}{2L}\int_{x_0}^{x_0+L}\left(\frac{\partial z}{\partial x}\right)^2 dx, \tag{2}$$

which represents the tension created by the stretching of the plate due to bending. The solution of (1) is obtained using an implicit finite difference method developed in [15] coupled with Newton's method to account for the nonlinear term N_x. Each panel is assumed clamped at both ends. The quantities p^+ and p^-, the pressures above and below the panels, are determined from the computation of the radiation and jet domains respectively.

The fluid equations are solved in conservation form. In terms of the vector

$$\hat{w} = (\rho, \rho u, \rho v, E)^T$$

the equations can be written in the form

$$\hat{w}_t + \hat{F}_x + \hat{G}_y = 0 \tag{3}$$

where subscripts denote derivatives, and the flux functions $\hat{F}$ and $\hat{G}$ are given by

$$\hat{F} = (\rho u, \rho u^2 + p, \rho uv, u(E+p))^T, \quad \hat{G} = (\rho v, \rho vu, \rho v^2 + p, v(E+p))^T$$

respectively. Here, ρ is the density, u, v are the x and y components of the velocity respectively and E is the total energy per unit volume,

$$E = \frac{1}{2}\rho(u^2+v^2) + c_v\rho T,$$

where T is the temperature and c_v is the specific heat per unit volume. The pressure, p, is obtained from the equation of state

$$p = \rho RT$$

where R is the gas constant. We note that the equations are solved separately in each domain. We do not distinguish the vector w in each domain for clarity.

We next restrict attention to the jet domain. Within this domain, the system (3) is modified to account for two different source terms

$$\hat{w}_t + \hat{F}_x + \hat{G}_y = \hat{s}_1(t,x,y) + \hat{s}_2(x,y). \tag{4}$$

The source term,

$$\hat{s}_1(t,x,y) = \epsilon f(t) g(x,y) \hat{w}_I, \tag{5}$$

serves as the starter pulse to excite the jet. Here, ϵ describes the amplitude of the source, $f(t)$ is a pulse which describes the time dependence of the source, $g(x,y)$ is a Gaussian peaked at a given location along the jet axis, and

$$\hat{w}_I = (1,\ U_0,\ 0,\ \frac{\gamma}{\gamma-1}p_\infty)^T$$

where the subscript "∞" denotes ambient quantities and $U_0(x, y)$ is a model describing a spreading jet profile taken from [19] in Cartesian coordinates. The vector w_I is chosen as follows. The component in the continuity equation serves as a mass injection. This is balanced by the component in the energy equation so that in the absence of flow and boundaries the solution remains homentropic. The component of the source in the axial momentum equation ensures that momentum is added to the system as the mass injected is convected downstream of the flow. The functional form of the pulse $f(t)$ is given by

$$f(t) = \exp(-at^2 - b/t^2), \tag{6}$$

with constants a and b. In the absence of flow and bounding surfaces, the solution would be a circular wave. As part of the validation of the numerical scheme, the computation with no flow has been extensively checked by grid refinement to give a convergent circular wave.

The second source term $\hat{s}_2(x, y)$ is designed so that in the absence of the starter pulse, i.e. $\epsilon = 0$, the solution to (4) would be a stationary profile corresponding to a spreading jet. The specified solution is

$$\hat{w}_0 = (\rho_\infty, \rho_\infty U_0, 0, \rho_\infty U_0^2/2 + c_v T_\infty)^T.$$

In the limit of small ϵ, the effect of the source term $\hat{s}_2$ leads to the Euler equations linearized about a spreading jet as in [21, 22] which by itself need not be a solution to the Euler equations. Incorporation of this term within the nonlinear Euler equations allows for the computation of nonlinear disturbances within the mean jet profile as in [2]. The inclusion of this source term separates the computation of the disturbance, in particular the resulting instability waves, from the computation of the mean flow (i.e., the spreading jet). Thus, the resulting system of equations allows for the simulation of instability waves and the resulting sound generation, together with the bending of acoustic waves in the jet flow field without requiring the computation of the spreading jet itself. Although this is a simplified model, the resulting system simulates many of the observed features of instability wave generated jet noise and permits high resolution computation of the coupling of jet noise with the flexible panels and the resulting radiation from the panels.

The initial conditions are taken to be the mean state $\hat{w}_0$ in the jet domain and ambient data in the radiation domain. The panels vibrate in response to excitation by sound from the jet as they would in an aircraft on the ground since the mean state corresponds to a static jet. Both the jet domain and the radiation domain are in principle unbounded regions. These domains are closed by the imposition of non-reflecting boundary conditions at the farfield boundaries, indicated in Figure 1. At these boundaries, we impose conditions designed to absorb outgoing circular waves [4]. Specifically we assume that the pressure has the functional form

$$p(t, x, y) \simeq h(c_\infty t - r, \theta)/\sqrt{r}, \tag{7}$$

where x and y are expressed in polar coordinates from a specified origin and c_∞ is the ambient sound speed. Differentiation of (7) with respect to t and r results in the relation

$$p_t + c_\infty p_r + (p - p_\infty)/(2r) = O(r^{-3/2}). \tag{8}$$

Neglecting the right hand side of (8) results in a radiation boundary condition which is effective in simulating outgoing waves provided the boundaries are sufficiently distant from all sources. We have verified that there are negligible boundary reflections for the data presented in this paper.

The Euler equations are solved using an explicit finite difference scheme which is fourth order accurate in the spatial coordinates and second order accurate in time. The scheme is a generalization

of the second order MacCormack scheme to allow higher order accuracy in space [10]. The numerical method has been validated on other problems of spatial instability. In particular, in [3] it was shown that the use of fourth order differencing can lead to a dramatic improvement in the calculation of growth rates for spatially unstable disturbances. In the numerical method we employ operator splitting in the two coordinate directions. The scheme is discussed in detail in other publications [21, 22].

3. Results

We consider a configuration as indicated in Figure 1. The jet exits from a straight nozzle of width $D = 2\text{in}$, assumed rigid on both the interior and exterior sides. The jet starter pulse (6) is located in the potential core at approximately $1.15D$ downstream of the nozzle exit on the axis of the jet. The constants a and b in (6) are $a = 3.4\,(c_\infty/D)^2$ and $b = 380\,(c_\infty/D)^{-2}$, chosen to give a frequency spectrum for f' within the range of interest for subsonic jets. An infinite wall is located approximately $6D$ above the jet and parallel to the nozzle. The wall is assumed rigid, except for two regions where flexible, aluminum, aircraft-type panels (panel A and panel B), with clamped boundaries are located. The panels are of length $5D$ and thickness $0.01D$ and are centered at $x = 0D$ and $x = 5.24D$ respectively. Other parameters of the panels are typical of aluminum. The origin of coordinates is chosen to be the horizontal location of the nozzle exit for x and the vertical location of the rigid wall for y. For the computations described below, we assume an exit flow Mach number of 0.65, with exit velocity $U_J = 0.65\,c_\infty$. Ambient conditions are assumed for ρ and p. Both the jet and radiation domain extend $48D$ downstream from $x = 0$, $12D$ in the upstream direction and $48D$ in the y direction. There are no detectable reflections from the artificial boundaries for the data presented here. We employ a grid of 351×351 points in the jet domain and 301×301 points in the radiation domain. The grid in the jet domain is stretched to improve resolution of the jet shear layer and source region. The solutions described here have been validated by grid refinement.

Our results are presented in three parts; the jet domain, including the flow and acoustic radiation from the jet, the responses of the panels and the acoustic radiation from the panels.

3a. Jet Flow Domain

Nonstationary behavior in the jet is triggered by the pulse starter, which generates a disturbance that propagates through the jet, interacts with the shear layer and then propagates into the farfield as sound. In the farfield this initial disturbance is non-circular due to convection. As a result of the interaction of the acoustic disturbance with the the shear layer gradient of the mean jet profile, instability waves are created. This was shown in [1], in the context of a linearization of (3). These waves are inviscid, a consequence of the fact that the Euler equations are employed in the computation. The instability waves propagate longitudinally along the jet at speeds less than the speed of sound, spreading transversally as does the mean flow. After an initial growth, their amplitude decays with the velocity as the jet spreads. As they propagate downstream they act as sources of additional disturbances as described in [17, 18, 26, 27, 29, 30] which propagate into the farfield as sound and also serve to excite further instability waves in the jet. This behavior is also consistent with experimental observations and with previous linear and nonlinear computations [2] and [22]. The resulting sound radiation forces the panels into a broadband response and radiation.

The acoustic radiation persists after the initial disturbance generated by the pulse starter has propagated a significant distance from the panels and away from the region of interest.

Figure 2 shows Power Spectral Densities (PSDs) of the farfield pressure (36D from the nozzle exit) for the case of a domain without any wall at 30°, 60°, and 90°. In order to help clarify the effects of the flow, the figure also includes the results for a computation without any flow (but with a nozzle) at 90°. We note that the no flow computation is not quite omni-directional due to scattering from the nozzle. We have verified that in the absence of the nozzle the no flow computation is omni-directional to a high degree of accuracy. This figure illustrates the role of the jet as an amplifier of sound. The acoustic farfield is least affected by the flow for angles near 90°, a result also demonstrated in [22]. The data at 30° shows two peaks, one near 700Hz. and another near 220Hz. The 700 Hz. peak corresponds to the peak frequency of the pulse, amplified due to the presense of flow as indicated by the large difference with respect to the no flow case. The 220Hz. peak results primarily from the shear noise generated from flow instabilities. Such a behavior was also observed in [2, 22] for axisymmetric jets. Low frequency peaks are also observed at 60°, although the amplitudes are reduced with respect to the pronounced low frequency peak at 30°. This figure illustrates that the computed sound radiation has features consistent with experimental observation.

The behavior of the resulting pressure field in the presence of the bounding wall, both within and outside of the flow, as well as the resulting acoustic radiation from the panels, is shown in Figures 3a-3e for successive values of time. Note that although both the jet and radiation domains in the computation extend $48D$ in y, the figures show solutions extended only to $30D$ in y in order to expand the visualization of the acoustic field. In interpreting these figures, note also that the actual levels assigned to each color for the jet and radiation domain differ so that different colors are assigned to the ambient regions. However, for each domain the values associated with the colors remain the same.

Figure 3a shows pressure contours at $t = 27.9D/c_\infty$, indicating the initial development of the unsteady jet flow and acoustic field of the jet and structure. There is a leading acoustic wave which propagates outside of the jet toward the farfield and toward the wall, as well as upstream both inside and outside the nozzle. As this wave reaches the wall, it reflects back and crosses the shear layer, trailing the initial disturbance, as shown in the figure. A large scale structure, related to the spatial instability of the jet shear layer is generated along the jet exit. This structure slowly propagates downstream. As a result of the interaction between the flexible panels with the pulse, the resulting vibration creates an acoustic disturbance which propagates into the radiation domain. In the jet flow field, as the process evolves, additional instability is created behind the initial leading wave as observed in the proximity of the nozzle exit. The pressure field is clearly asymmetric about the jet axis due to the presence of the wall.

As the time evolves (Figure 3b) additional pressure waves are created from the jet instability which propagate into the farfield. Figures 3b-3e show the evolution of the instability wave as it propagates downstream. The additional sound generated from this large scale structure can also be seen by following the progression of the leading acoustic wave in Figures 3b-3d. While the initial waves due to the starter pulse exit the computational domain (Figure 3d), additional instability waves continue to be generated within the jet shear layer, together with the associated shedding of acoustic disturbances from the nozzle lip. Hence, long after the initial waves generated by the pulse starter have propagated far downstream from the region of interest, indeed, after they have exited the domain, sound is continually generated which results in a continual excitation of the panels.

In addition, Figures 3a-3e show waves propagating between the pipe and wall boundary, upstream of the nozzle exit. The behavior described above has also been verified by a detailed animation of successive contours generated by the computation.

In Figure 4 we illustrate the shedding of disturbances from the nozzle lip. The figure shows the pressure in a small region around the nozzle lip for three closely spaced values of time. In the top illustration, corresponding to the earliest time, the formation of a pressure disturbance at the upper lip of the nozzle exit can be seen. The middle illustration, at a slightly later time, shows that this disturbance has shed from the upper lip, while a new disturbance is being generated at the lower lip. In the bottom illustration, the disturbance has shed from the lower lip, while a new disturbance is forming at the upper lip. The figure illustrates the alternating shedding of pressure disturbances from both sides of the nozzle. This behavior is consistent with experimental observations [12] and is a source of sound forcing the panels to vibrate. A similar phenomenon was found in the axisymmetric computations [21]. Note that for the axisymmetric case, ring type of disturbances can be shed from the nozzle lip. The figures also illustrate the propagation of disturbances up the pipe.

3b. Responses of the Panels

We first consider the PSD of the pressure incident on the centers of each panel. In order to clarify the mechanisms influencing the spectral content, we compare the results to a computation without flow, in which panel excitation occurs from the starter pulse, as well as to a computation with flow but without a bounding wall. The data are presented in Figures 5a and 5b for panels A and B respectively.

Figure 5a shows that the PSDs of the incident pressure on panel A for the wall/flow computation are comprised of relatively discrete spectral bands. The behavior for the wall/no flow computation exhibits similar discrete bands with lower amplitude levels. In contrast, the computation of no wall/flow exhibits a continous smooth spectrum. Thus, the discrete spectral bands exhibited for the wall/flow and wall/no flow computations appear to be a direct consequence of repeated reflections between the wall and the nozzle. Note that the no wall/flow spectrum is similar to that of the farfield pressure at 90° (Figure 2). This is a consequence of the spatial location of panel A relative to the nozzle exit.

The PSDs of the pressure incident on panel B with and without flow exhibit much greater differences in comparison to those for panel A. In particular, the flow computations exhibit significant amplification of low frequencies as compared to the no flow computation. This low frequency amplification is due to sound generated by instabilities within the flow. Note that the PSD of the no wall/flow case is similar to that of the farfield pressure at 30° (Figure 2), a consequence of the fact that the center point of panel B is nearly 39° from the nozzle exit. The wall/flow computation exhibits discrete spectral bands for higher frequencies. We interpret this behavior as due to repeated reflections between the wall and the jet boundary. The wall/no flow computation exhibits a significantly less pronounced band structure, presumably due to the fact that there is now no direct mechanism to promote repeated reflections at the wall.

Since the panels are identical in all respects, these results indicate that the loading on the panels depends very crucially on the geometric placing of the panels relative to the nozzle exit.

The enhanced low frequency loading on panel B, due to instability wave generated sound, is in a frequency band for which the panel can be readily excited. As will be seen, this enhanced loading

is reflected in enhanced vibration of and radiation from panel B. We note that these results also indicate that near the wall rapid variations in x occur in the unsteady pressure near the nozzle exit.

The effect of the enhanced low frequency excitation of panel B can be seen in Figures 6 and 7 where we plot the PSD for the panel velocities and transmitted pressure respectively at the panel centers. Both panels exhibit relatively narrow, nearly coincident bands of peak spectral response. We denote these bands for the velocity spectra by β_{v1}, β_{v2}, β_{v3} and for the transmitted pressure spectra by β_{p1}, β_{p2}, β_{p3}. The enhanced low frequency response of panel B is apparent from both figures. In view of the analysis of the incident pressure above we attribute this enhanced response primarily to instability wave generated sound which provides enhanced excitation of the downstream panel B. We note that the broadband incident pressure on panel B is converted to a discrete velocity and transmitted pressure spectra. The three primary pressure bands, β_{p1}, β_{p2}, β_{p3}, are clearly associated with the analogous velocity bands, β_{v1}, β_{v2}, β_{v3}. The large response for panel B in the band β_{v2}, together with the associated radiation (β_{p2}), represent the main effect of the instability wave generated sound on the panels and reflects the frequencies within the broadband indicated in Figure 5b at which the panel is most responsive.

The results indicate the role of panels located downstream of the jet exit as a narrow filter, converting a broadband forcing into relatively narrow spectral bands. The bands are concentrated in the low frequency range, characteristic of instability wave generated sound, which indicates that shear layer instabilities can be an important mechanism in panel excitation.

3c. Acoustic Radiation from the Panels

The time evolution of the pressure radiated by the motion of the panels is shown at successive times in Figures 3a-3e. Figure 3a shows a nearly circular leading wave radiating away from the panels. This is due to the excitation of the panels by the leading acoustic disturbance initiated by the pulse starter. In addition, there is an asymmetrical disturbance generated primarily from panel B which propagates mainly in the downstream direction (Figure 3b).

As time evolves, repeated radiation from both panels occurs. The figures clearly demonstrate a preferred downstream beaming of this radiation, although there is noticeable upstream acoustic generation as well. This is in contrast to the nearly circular disturbance generated by the pulse starter. We note the presence of well defined radiation even at late times, after the initial disturbance due to the pulse starter has exited the computational domain.

PSDs of the radiated pressure at sample farfield points are shown in Figure 8. Results are presented along the line $y = 36D$ for selected values of x. The farfield spectra exhibit relatively discrete spectral bands. The three pronounced frequency bands ($\tilde{\beta_{p1}}$, $\tilde{\beta_{p2}}$, $\tilde{\beta_{p3}}$), are analogous to those for the velocity and transmitted pressure (Figures 6 and 7). The primary feature of the radiation is the presence of the large peak ($\tilde{\beta_{p1}}$) near 250 Hz. This is an effect of the flow and, based on the transmitted pressure (for example, Figure 7), is primarily due to radiation from the downstream panel (panel B). We note that while the panels can be most readily excited at low frequencies, the comparable peak in a computation with no flow is roughly three times smaller than the peak indicated in Figure 8. Thus, the low frequency spike is a consequence of low frequency sound generation within the flow field. The enhanced radiation corresponding to this peak is primarily a manifestation of the excitation of the panels by instability wave generated sound.

4. Conclusion

We have computed the full flow/acoustic/structure coupling for a model of a panel-stringer assembly forced by jet noise. The jet is initially excited by a pulse and continues radiating sound long after the initial disturbance due to the pulse has exited the computational domain, thus simulating the behavior of a real jet flow field. This radiation is due to the triggering of instability waves in the jet. The instability waves act as sources of sound, generating directionally beamed low frequency sound into the farfield primarily at low to mid angles to the jet axis. Instability wave generated sound acts to excite the flexible panels, particularly the panel located downstream of the nozzle exit. Thus, the location of the panels with respect to the jet exit is critical in terms of the resulting structural vibration and acoustic radiation.

The panels act as a narrow filter, converting the relatively broadband incident pressure to a transmitted pressure exhibiting relatively narrow spectral bands. The narrow spectral bands are also present in the far field radiation from the panels. The radiation from the panels is beamed primarily downstream and vertically from the panels. The frequencies of the radiated pressure are related both to properties of the panels and to the properties of the incident forcing pressure, which in turn is dependent on the shear layer instabilities of the jet. Due to a continual excitation of instabilities in the jet, radiation persists long after the initial disturbance generated by the pulse exits the computational domain.

Acknowledgements

The authors thank Dr. Jay Hardin for helpful discussions and comments.

References

[1] Bayliss, A., and Maestrello, L., " Simulation of Instabilities and Sound Radiation in a Jet," *AIAA Journal*, Vol. 19, 1981, pp. 835-841.

[2] Bayliss, A., Maestrello, L., and Turkel, E., "On the Interaction of a Sound Pulse With the Shear Layer of an Axisymmetric Jet, III: Non-Linear Effects", *Journal of Sound and Vibration*, Vol. 107, 1986, pp. 167-175.

[3] Bayliss, A., Parikh, P., Maestrello, L., and Turkel, E., "A Fourth Order Scheme For the Unsteady Compressible Navier-Stokes Equations," AIAA paper 85-1694, 1985.

[4] Bayliss, A., and Turkel, E., "Far-Field Boundary Conditions For Compressible Flows," *Journal of Computational Physics*, Vol. 48, 1982, pp. 182-199.

[5] Bechert, D.W., and Pfizenmaier, E., "On the Amplification of Broadband Jet Noise by Pure Tone Excitation," *Journal of Sound and Vibration*, Vol. 43, 1975, pp. 581-587.

[6] Blevins, R.D., "An Approximate Method for Sonic Fatigue Analysis of Plates and Shells," *Journal of Sound and Vibration*, Vol. 129, 1989, pp. 51-71.

[7] Crow, S., and Champagne, F., "Orderly Structure in Jet Turbulence," *Journal of Fluid Mechanics*, Vol. 48, 1971, pp. 457-591.

[8] Dowell, E. H/, "Transmission of Noise from a Turbulent Boundary Layer through a Flexible Plate into a Closed Cavity", *Journal of the Acoustic Society of America*, Vol. 46, 1969, pp. 238-252.

[9] Frendi, A., Maestrello, L., and Bayliss, A., "Coupling Between Plate Vibration and Acoustic Radiation," to appear in the *Journal of Sound and Vibration.*

[10] Gottlieb, D., and Turkel, E., "Dissipative Two-Four Methods For Time-Dependent Problems," *Mathematic Computation*, Vol. 30, 1976, pp. 703-723.

[11] Hardin, J.C., "Introduction to Time Series Analysis," NASA Reference Publication 1145, NASA Langley Research Center, 1990.

[12] Ho, C. M. and Huang, L. S., "Subharmonics and Vortex Merging in Mixing Layers", *Journal of Fluid Mechanics*, Vol. 119, 1982, 443-473.

[13] Huerre, P., Monkewitz, P.A., "Absolute and Convective Instabilities in Shear Layers." *Journal of Fluid Mechanics*, Vol. 159, 1985, pp. 151-168.

[14] Huerre, P., Monkewitz, P.A., "Local and Global Instabilities in Spatially-Developing Flows", Ann. Rev. Fluid Mech., Vol. 22, 1990, pp. 473-537.

[15] Hoff, C., and Pahl, P.J., "Development of an Implicit Method With Numerical Dissipation From a Generalized Single-Step Algorithm For Structural Dynamics," *Computer Methods in Applied Mechanics and Engineering 67*, 1988, pp. 367-385, North-Holland.

[16] Kibens, V., "Discrete Noise Spectrum Generated by an Acoustically Excited Jet," *AIAA Jounal*, Vol. 18, 1980, pp. 434-441.

[17] Lighthill, M.J., "On Sound Generated Aerodynamically-I, General Theory," *Proceedings of the Royal Society*, Vol. A222, 1954, pp. 1-32.

[18] Lilley, G.M., "Theory of Turbulence Generated Jet Noise: Generation of Sound in a Mixing Region," *U.S. Air Force Technical Report AFAPL-TR-72-53*, **IV**.

[19] Maestrello, L., "Acoustic Energy Flow From Subsonic Jets and Their Mean and Turbulent Flow Structure," *Ph.D. Thesis, University of Southampton*, 1975.

[20] Maestrello, L., "Active Control of Nonlinear-Nonstationary Response and Radiation of a Panel-Stringer Structure Near a Supersonic Jet," AIAA 93-4338, 1993.

[21] Maestrello, L., and Bayliss, A., "Flowfield and Far Field Acoustic Amplification Properties of Heated and Unheated Jets," *AIAA Journal*, Vol. 20, 1982, pp. 1539-1546.

[22] Maestrello, L., A. Bayliss and E. Turkel, "On the Interaction of a Sound Pulse with the Shear Layer of an Axisymmetric Jet," *Journal of Sound and Vibration*, Vol. 74, 1981, pp. 281-301.

[23] Maestrello, L., Frendi, A., and Brown, D.E., " Nonlinear Vibration and Radiation from a Panel With Transition to Chaos," *AIAA Journal*, Vol. 30, No. 11, 1992, pp. 2632-2638.

[24] Maestrello, L., and Pao, S. P., "New Evidence of the Mechanisms of Noise Generation and Radiation of a Subsonic Jet," *Journal of Acoustical Society of America*, Vol. 57, No. 4, 1975, pp. 959-960.

[25] Mankbadi, R., Hayder, M., and Povinelli, L., "The Structure of Supersonic Jet Flow and Its Radiated Sound," AIAA Paper 93-0549, 1993.

[26] Michalke, A., and Hermann G. "On the Inviscid Instability of a Circular Jet With External Flow", *Journal of Fluid Mechanics.*, Vol. 114, 1982, 343-359.

[27] Michalke, A., "Survey on Jet Instability Theory", *Progr. Aerospace Sci.*, Vol. 21, 1984, pp. 159-199.

[28] Phillips, O.M., "The Irrotational Motion Outside the Free Turbulent Boundary," *Proceedings of the Cambridge Philosophical Society*, Vol. 51, 1955, pp. 222-229.

[29] Ribner, H.S., Dryden Lecture Perspectives on Jet Noise, *American Institute of Aeronautics and Astronautics Journal,* Vol. 19, 1981, pp. 1513-1526.

[30] Tam, C.K.W., "Jet Noise Generated by Large-Scale Coherent Motion," Chapter 6 in Aeroacoustics of Flight Vehicles, Theory and Practice, Vol. 1, 1991, Edited by H.H. Hubbard.

[31] Tam, C.K.W., and Morris, P.J., "The Radiation of Sound by the Instability of a Compressibly Plane Turbulent Shear Layer," *Journal of Sound and Vibration*, Vol. 102, 1985, pp. 129.

[32] Ting, L., " On-surface Conditions for Structural Acoustic Interactions in Moving Media." Presented at the Workshop on Perturbation Methods in Physical Mathematics. Rensselaer Polytechnic Institute, Troy, NY, June 23-26, 1993.

[33] Ting, L. and Miksis M. J., "On vortical flow and sound generation," *SIAM J. Appl. Math.*, Vol. 50, 1990, pp. 521-536.

[34] Vlasov, YE. V., and Ginevsky, A.S., "Generation and Suppression of Turbulence in an Axisymmetric Turbulent Jet in the Presence of an Acoustic Influence," *ANASA TT-F15*, 1974, p.721.

[35] Wang, T., "Dynamic Forcing Function for Flow-Acoustic-Induced Vibration,"*Journal of Pressure Vessel Technology*, Vol. 111, 1989, pp.361-370.

Fig. 1 Computational Domain

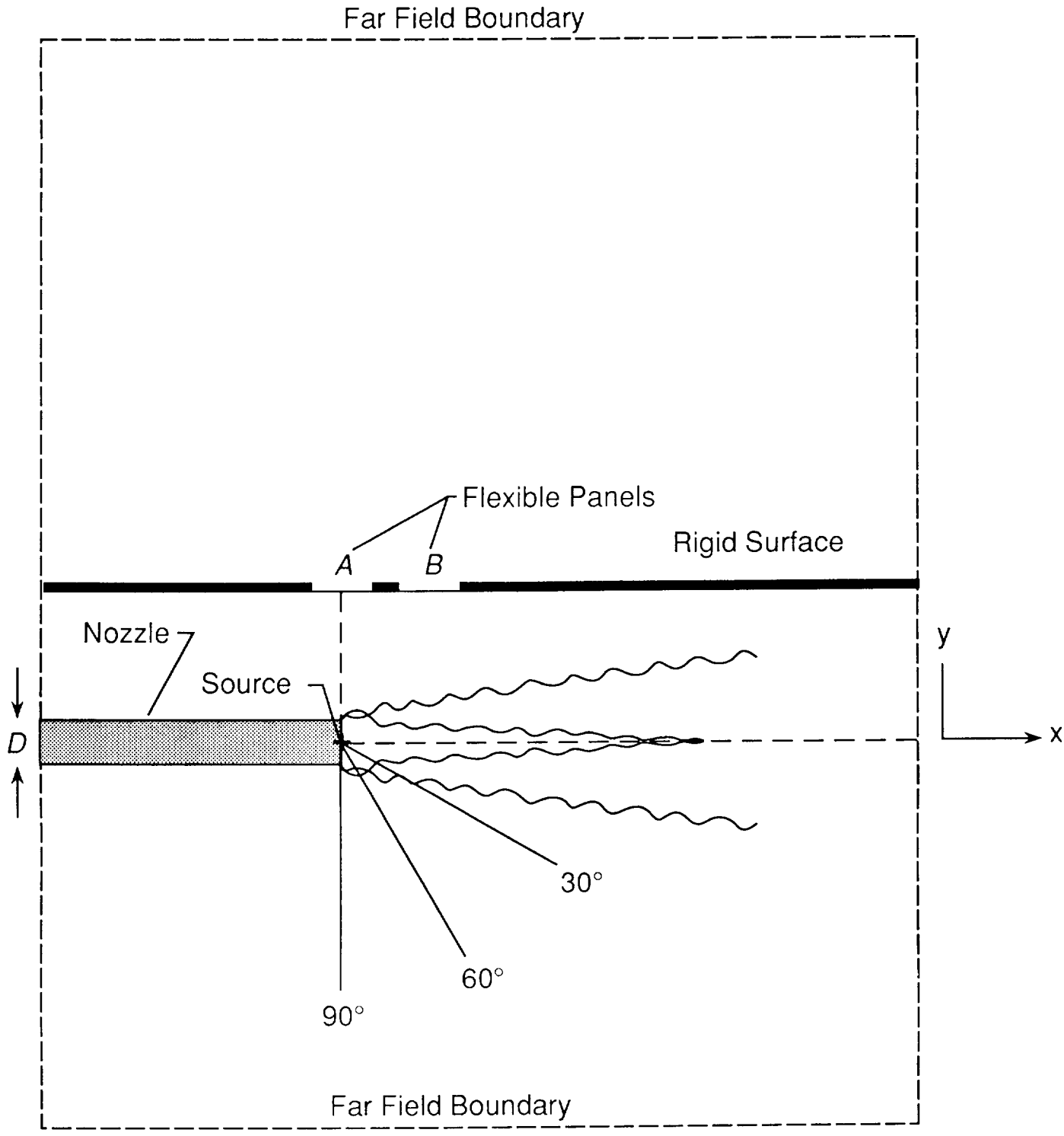

Fig. 2 PSD of farfield $p-p_\infty$ on a circle of radius $r = 20D$ at $30°, 60°, 90°$ in a domain with no bounding walls

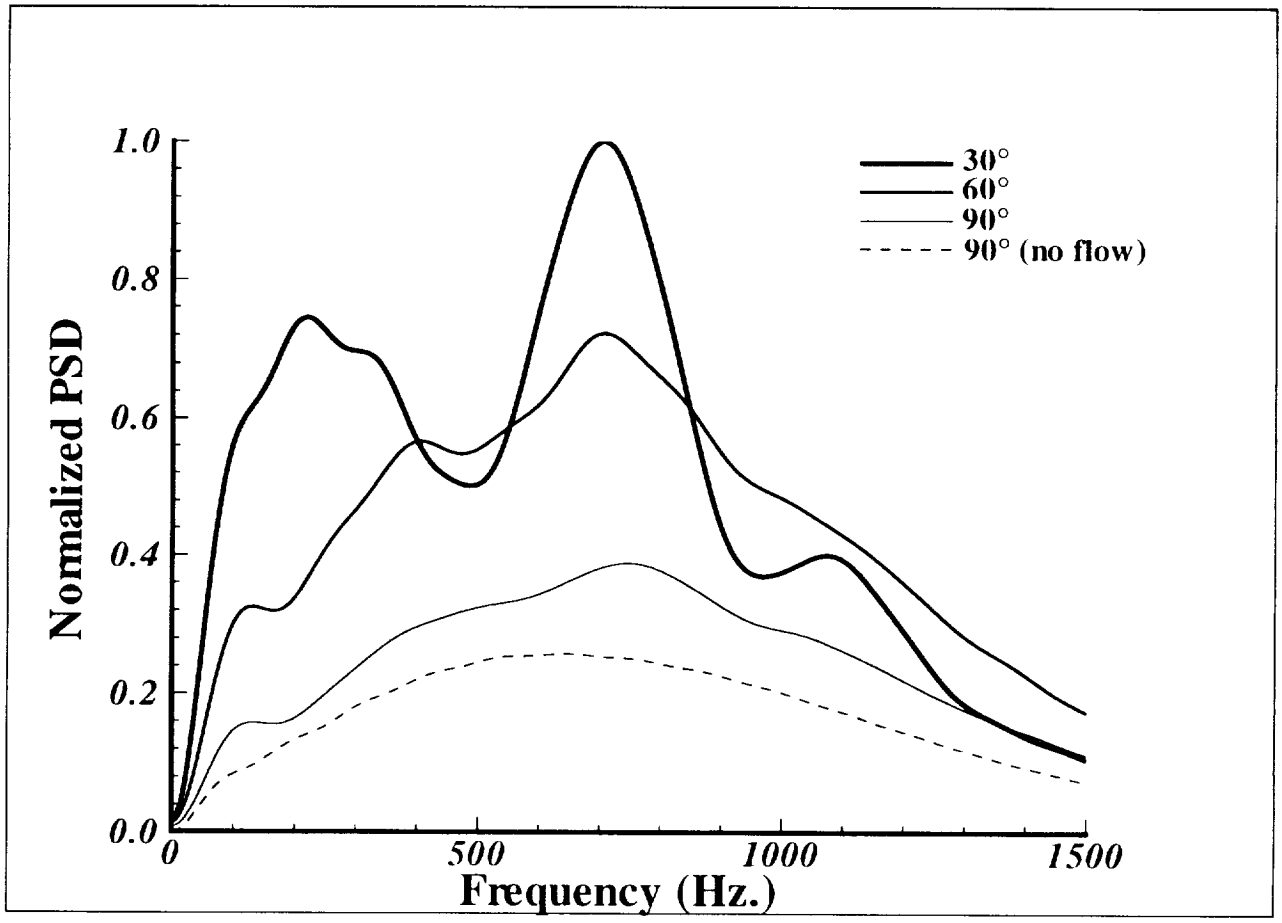

Fig. 3 Contours of constant $p-p_\infty$ at successive times

(a)$t = 27.9D/c_\infty$

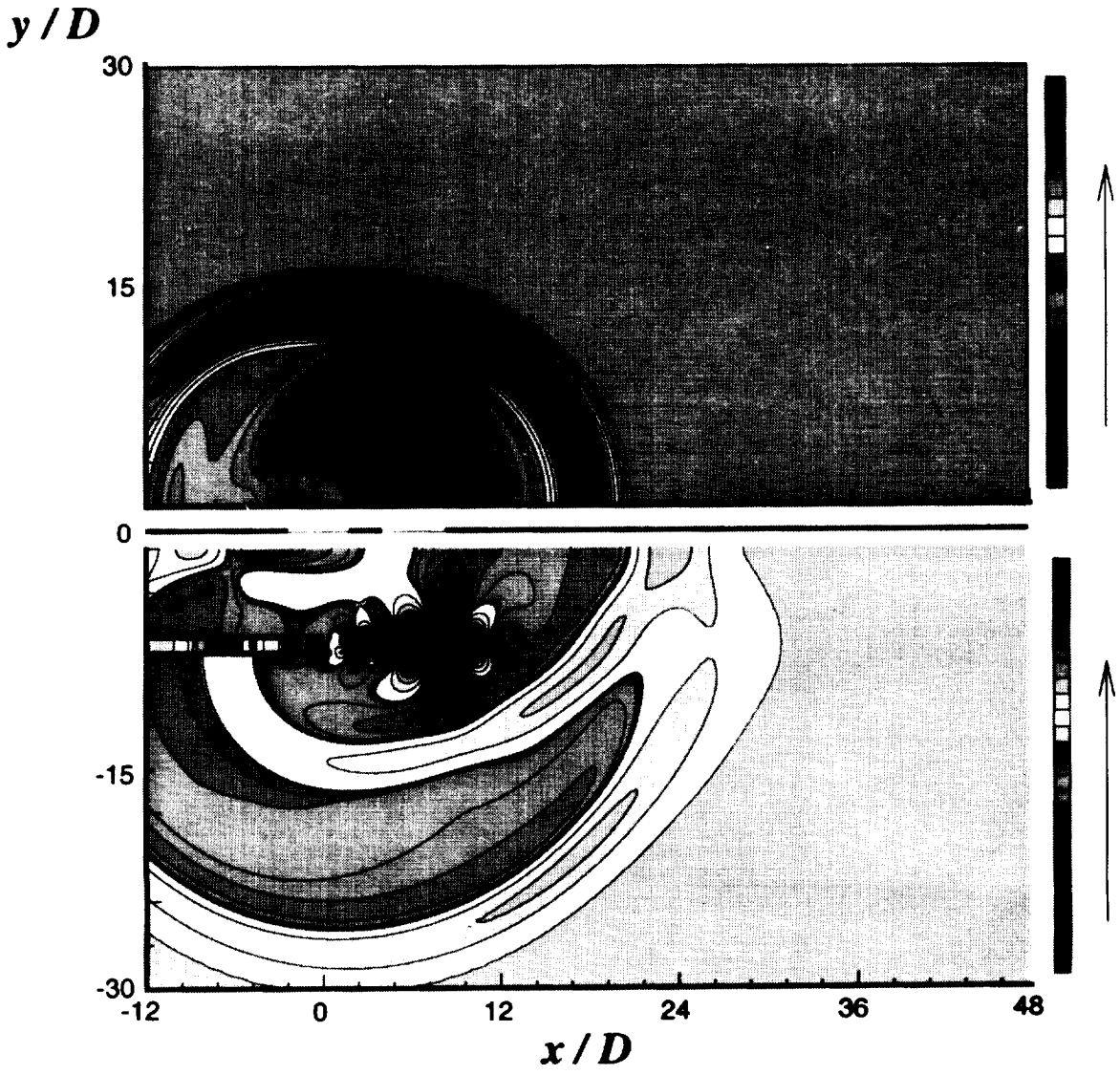

Fig. 3 Contours of constant $p-p_\infty$ at successive times

(b)$t = 38.4D/c_\infty$

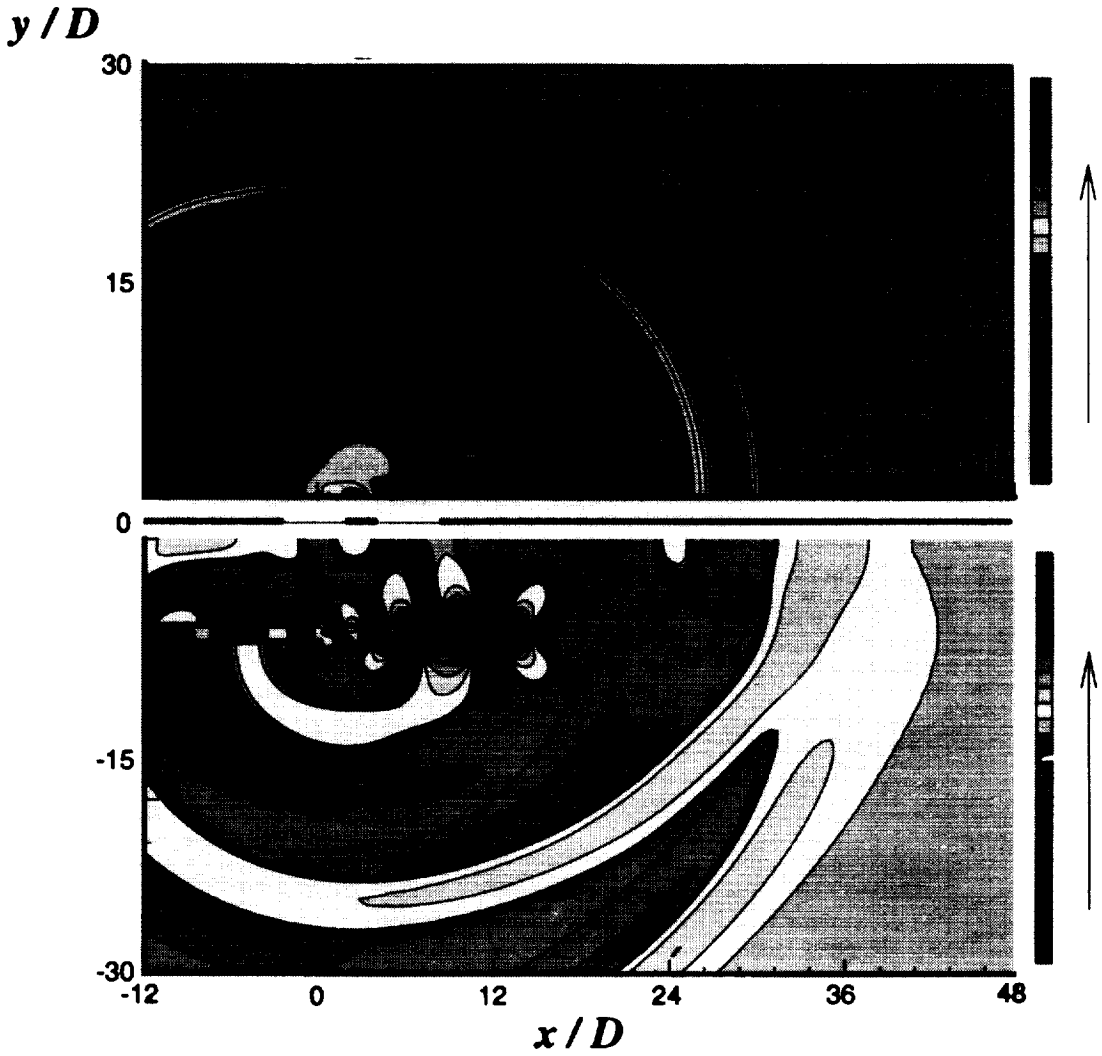

Fig. 3 Contours of constant $p-p_\infty$ at successive times

$(c)t = 45.3D/c_\infty$

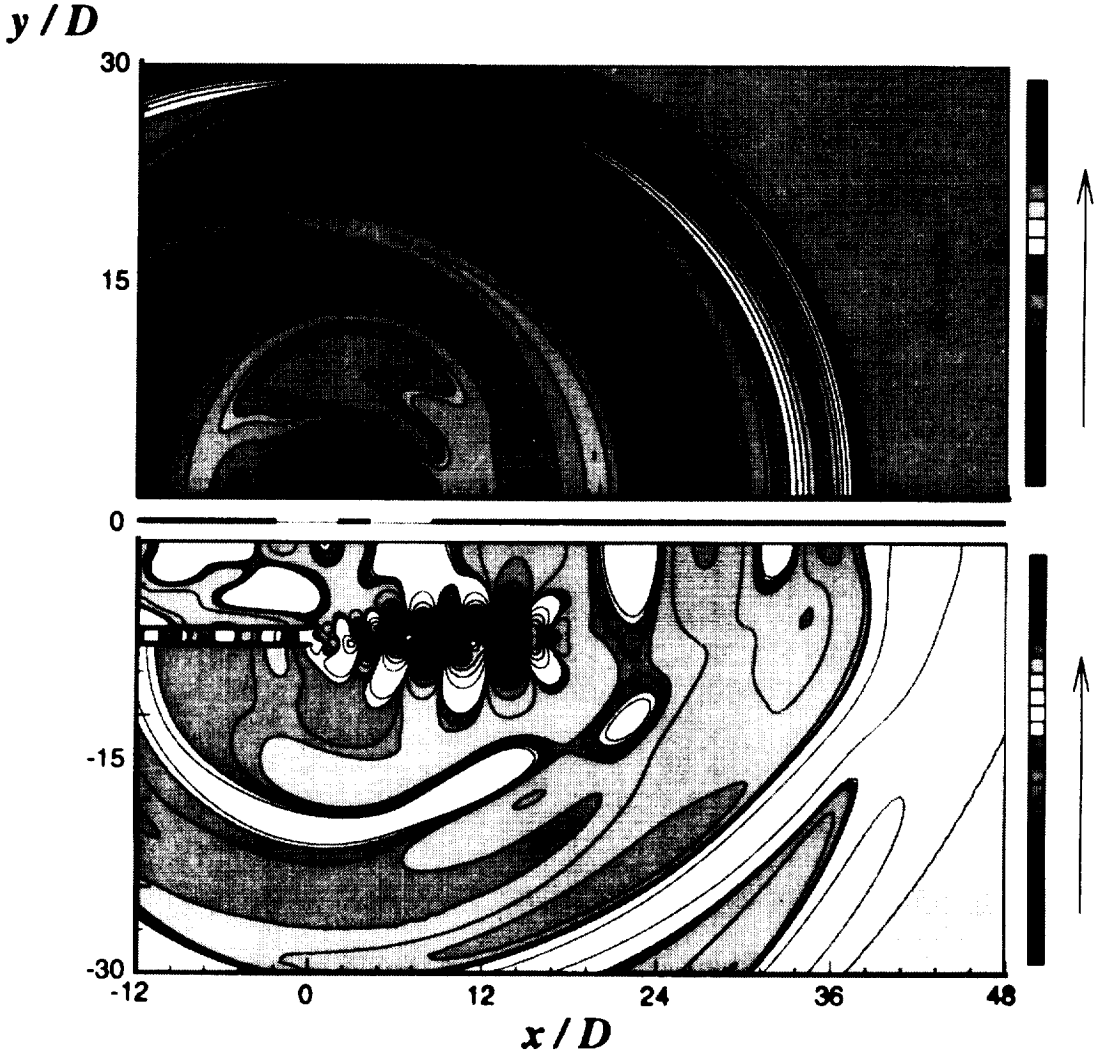

Fig. 3 Contours of constant $p-p_\infty$ at successive times

(d)$t = 62.8D/c_\infty$

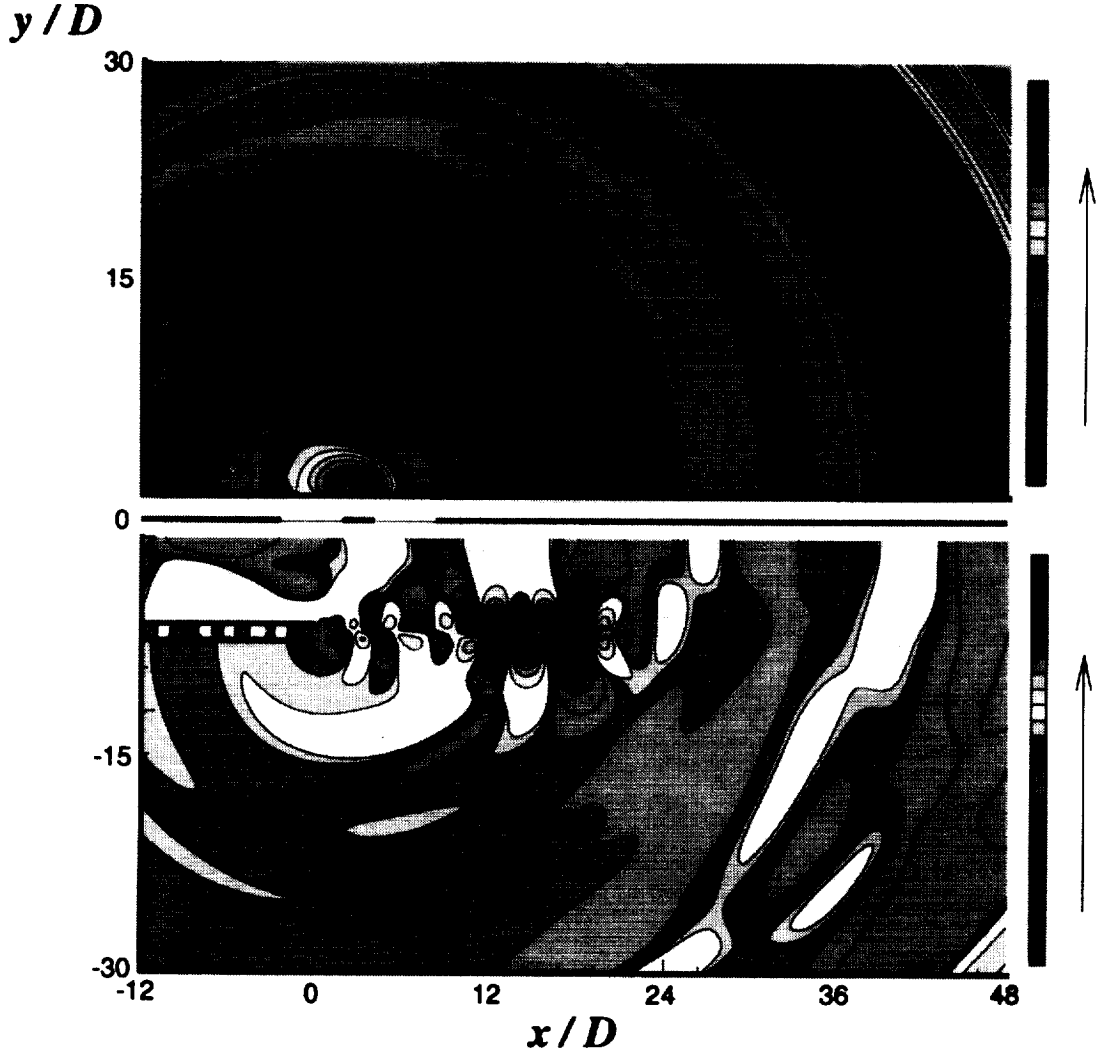

Fig. 3 Contours of constant $p-p_\infty$ at successive times

(e)$t = 73.3D/c_\infty$

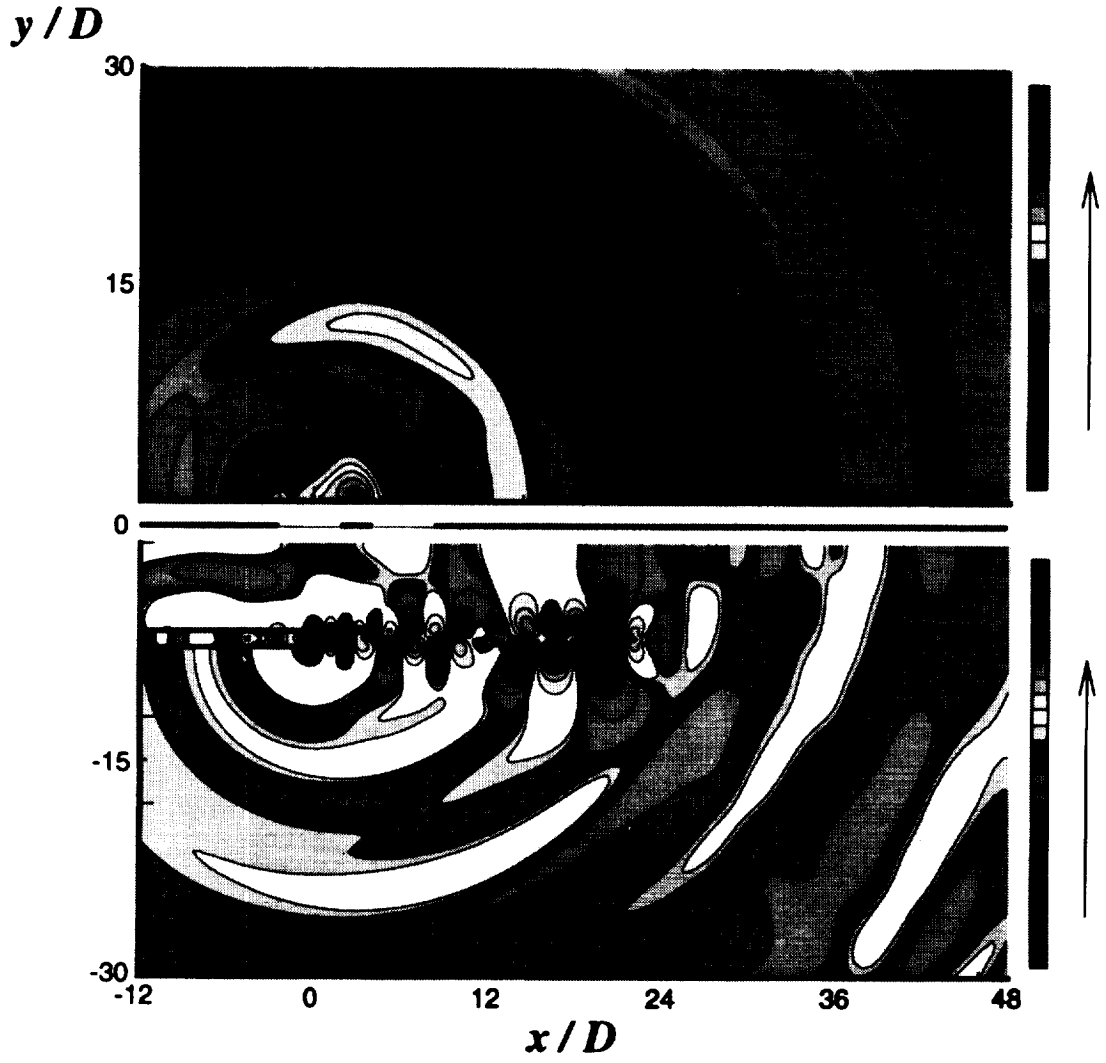

Fig. 4 Evolution of pressure disturbances shed from the nozzel at 3 successive times (from top to bottom) $t = 34.9D/c_\infty$, $t = 36.6D/c_\infty$, $t = 38.4D/c_\infty$. An expanded region about the nozzle lip is shown.

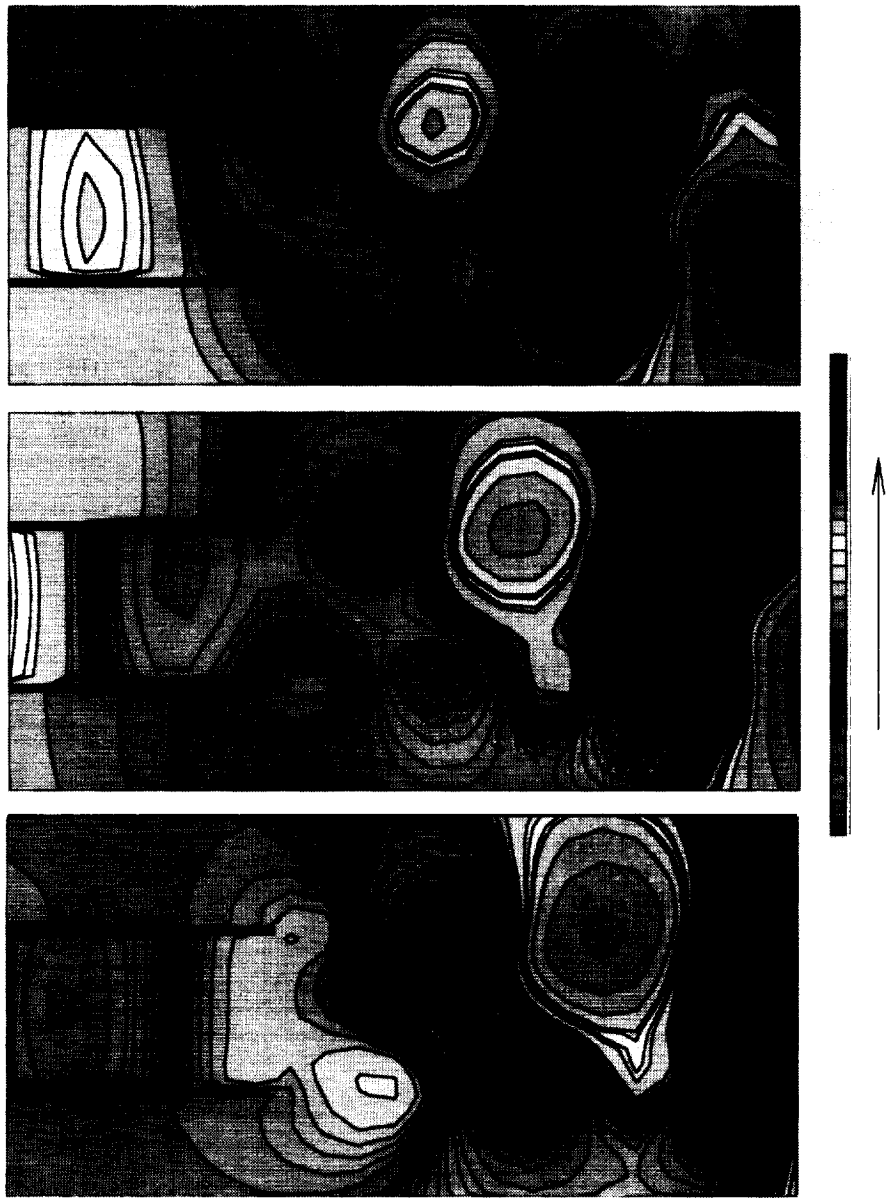

Fig. 5 PSD of incident $p - p_\infty$ at the center of (a) panel A.

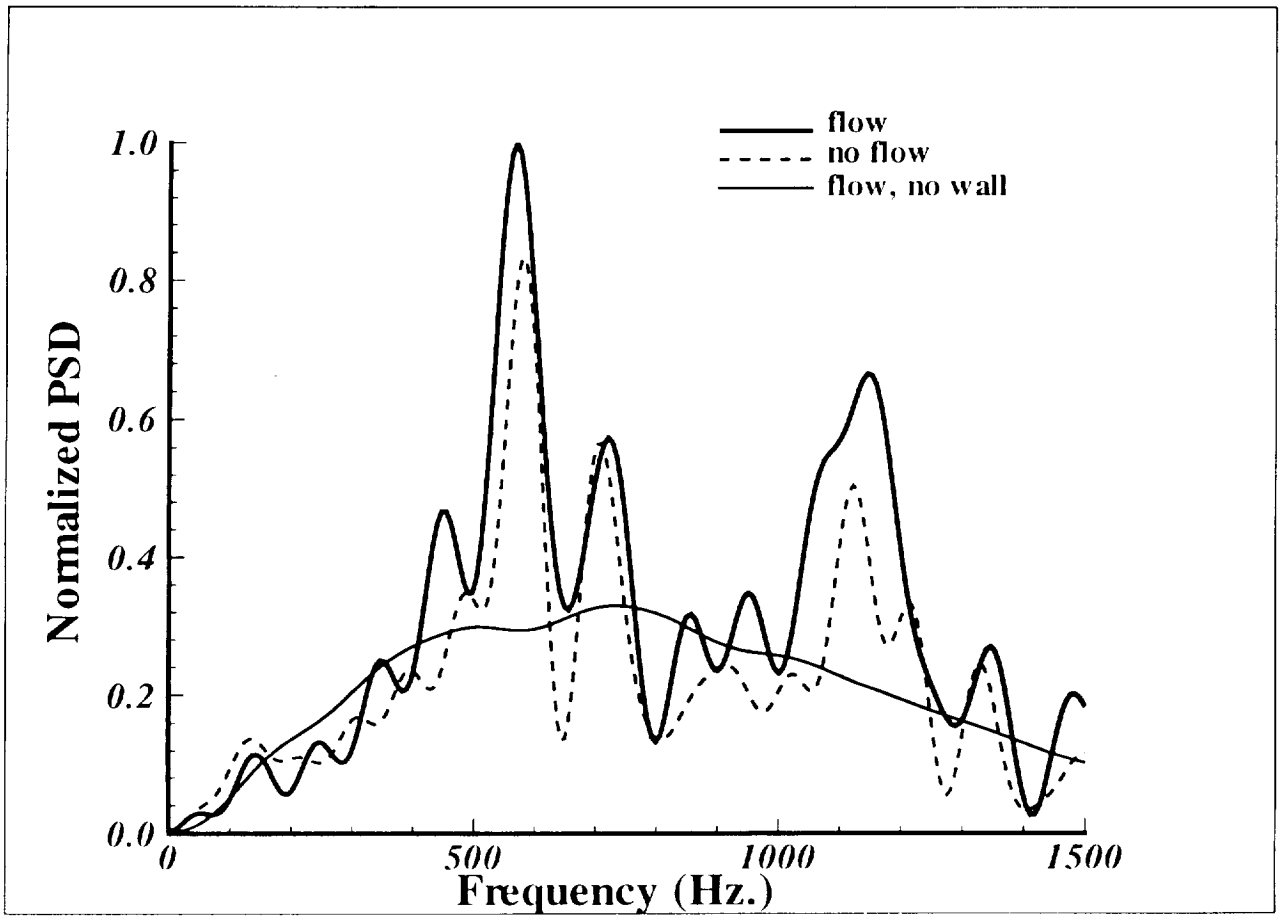

Fig. 5 PSD of incident $p - p_\infty$ at the center of (b) panel B for the computations of wall/flow, wall/noflow and no wall/flow.

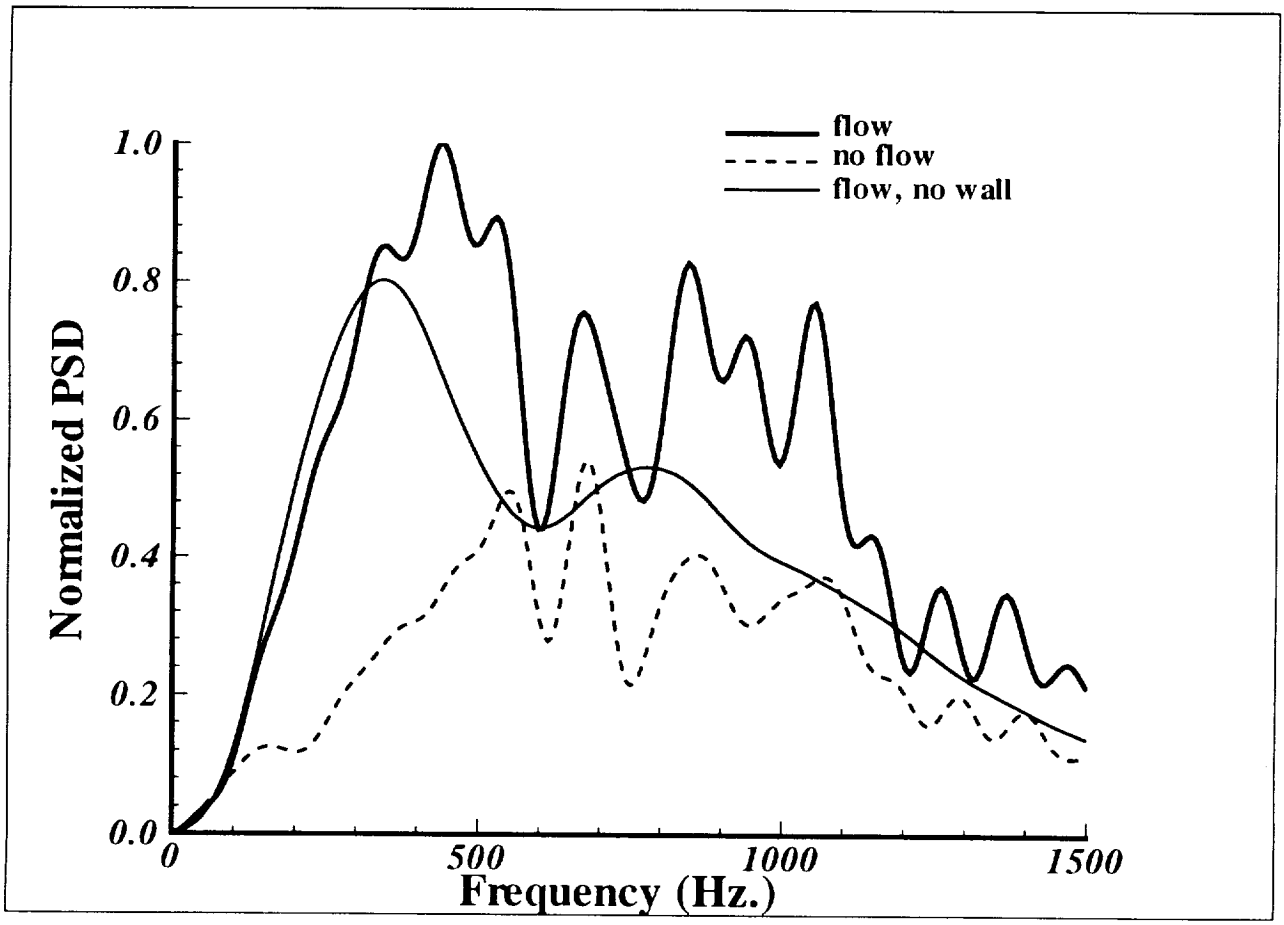

Fig. 6 PSD of v at panel centers

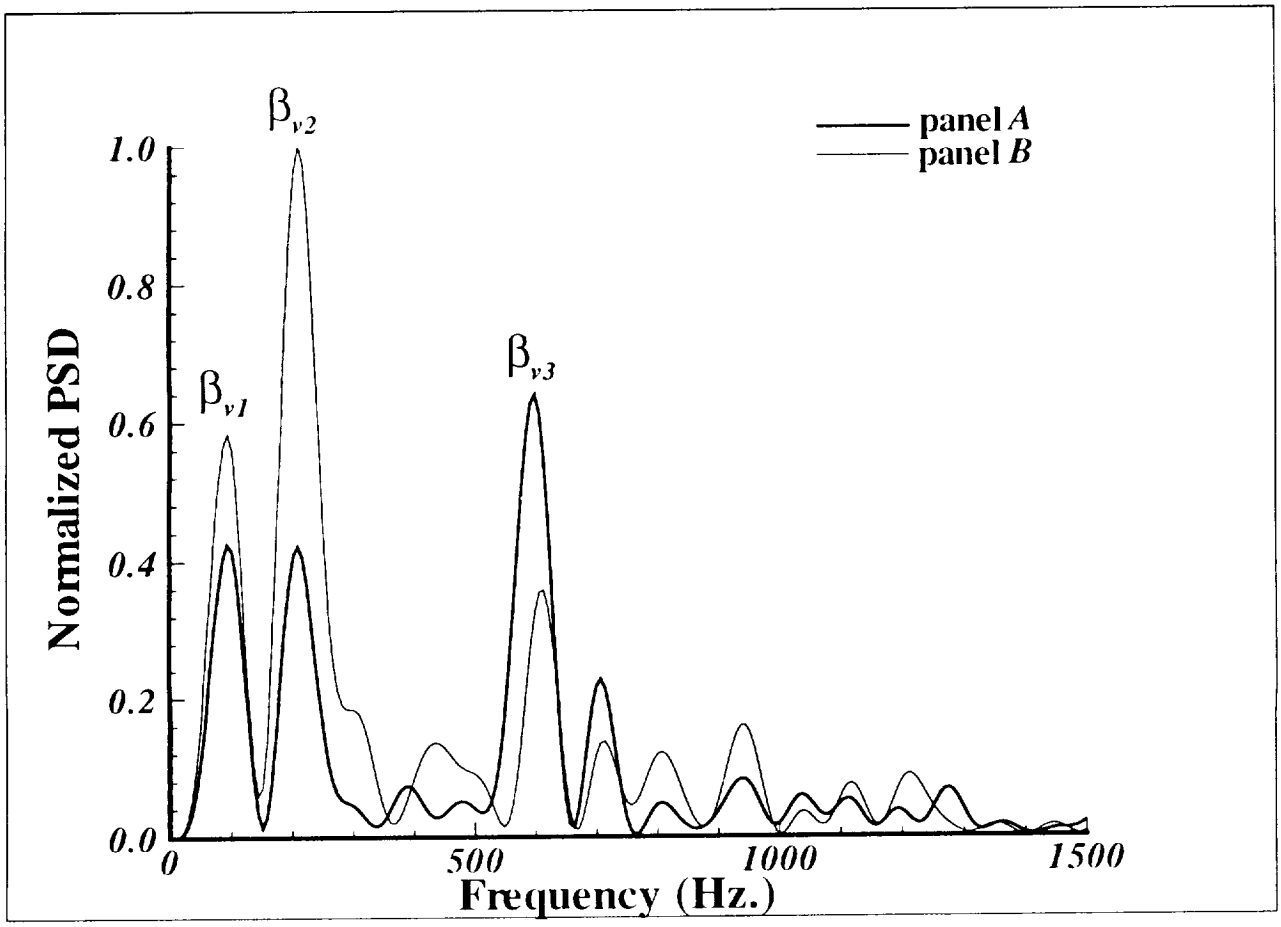

Fig. 7 PSD of transmitted pressure

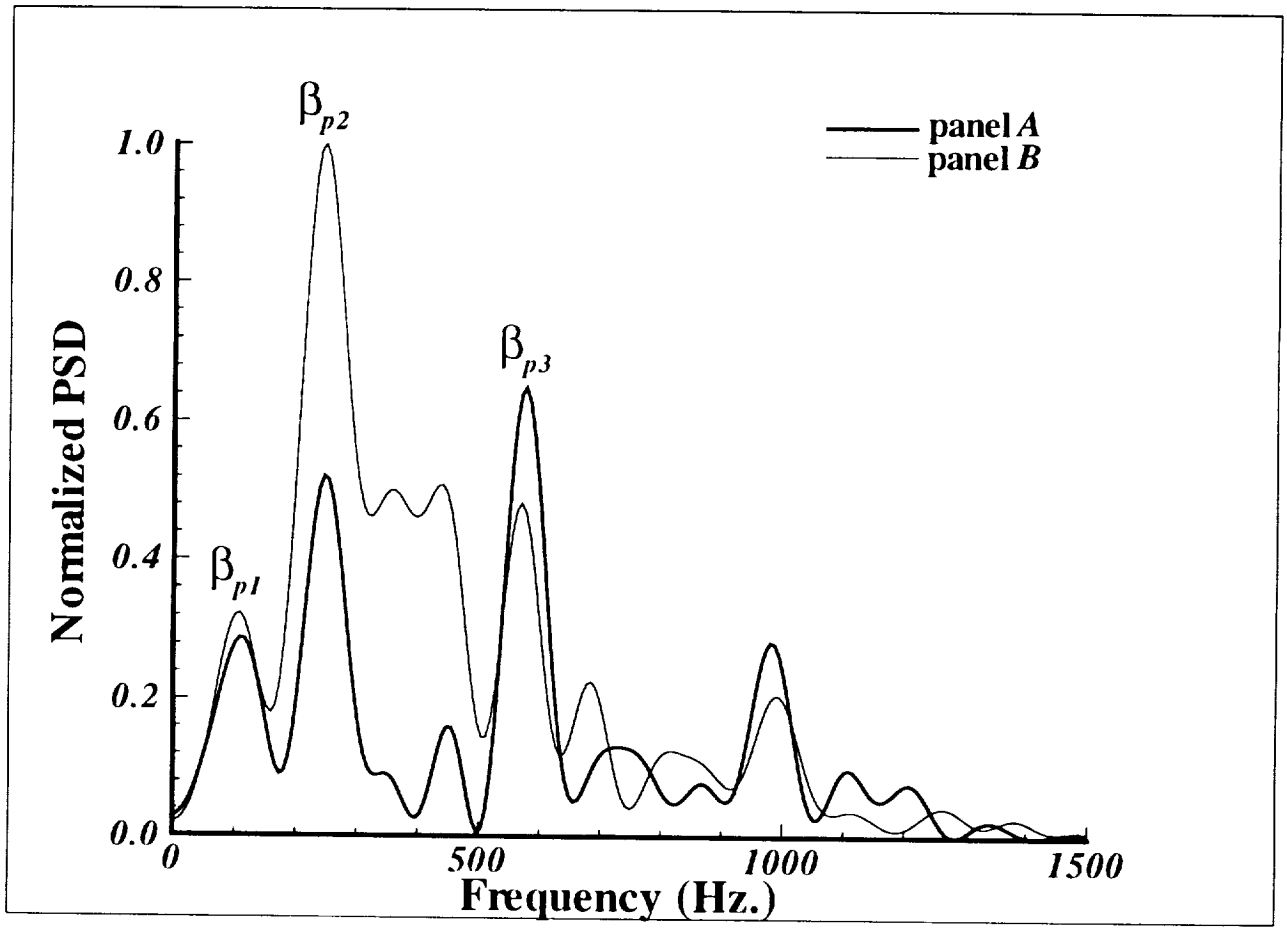

Fig. 8 PSD of radiated $p - p_\infty$ at

$x = -12D, x = 6D, x = 18D$, along the line $y = 36D$.

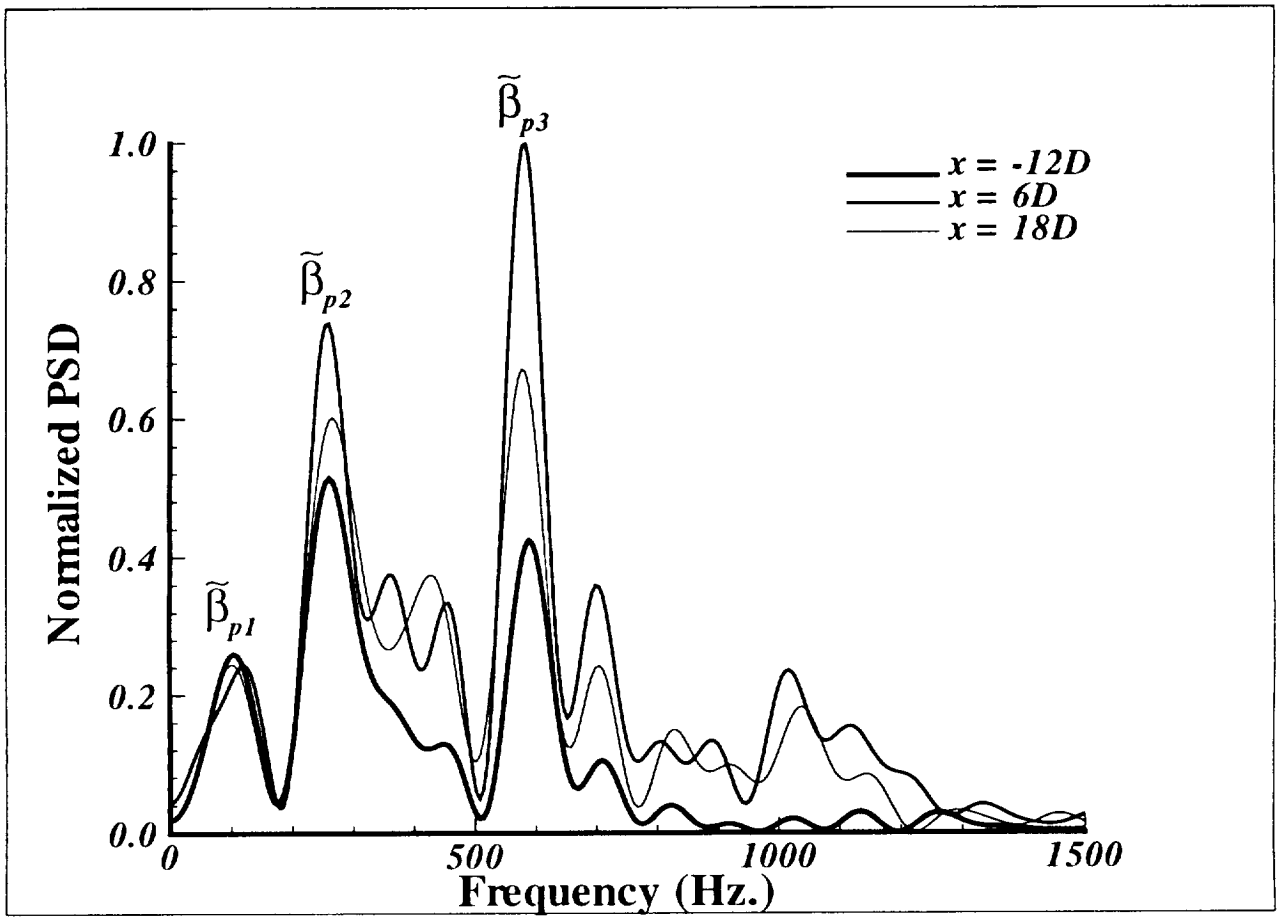

REPORT DOCUMENTATION PAGE

Form Approved
OMB No. 0704-0188

1. AGENCY USE ONLY *(Leave blank)*	2. REPORT DATE	3. REPORT TYPE AND DATES COVERED
	June 1994	Contractor Report

4. TITLE AND SUBTITLE
ON THE INTERACTION OF JET NOISE WITH A NEARBY FLEXIBLE STRUCTURE

5. FUNDING NUMBERS
C NAS1-19480
WU 505-90-52-01

6. AUTHOR(S)
J. L. McGreevy
A. Bayliss
L. Maestrello

7. PERFORMING ORGANIZATION NAME(S) AND ADDRESS(ES)
Institute for Computer Applications in Science
and Engineering
Mail Stop 132C, NASA Langley Research Center
Hampton, VA 23681-0001

8. PERFORMING ORGANIZATION REPORT NUMBER
ICASE Report No. 94-48

9. SPONSORING/MONITORING AGENCY NAME(S) AND ADDRESS(ES)
National Aeronautics and Space Administration
Langley Research Center
Hampton, VA 23681-0001

10. SPONSORING/MONITORING AGENCY REPORT NUMBER
NASA CR-194934
ICASE Report No. 94-48

11. SUPPLEMENTARY NOTES
Langley Technical Monitor: Michael F. Card
Final Report
Submitted to AIAA Journal

12a. DISTRIBUTION/AVAILABILITY STATEMENT
Unclassified–Unlimited
Subject Category 34

12b. DISTRIBUTION CODE

13. ABSTRACT *(Maximum 200 words)*

The model of the interaction of the noise from a spreading subsonic jet with a panel-stringer assembly is studied numerically in two dimensions. The radiation resulting from this flow/acoustic/structure coupling is computed and analyzed in both the time and frequency domains. The jet is initially excited by a pulse-like source inserted into the flow field. The pulse triggers instabilities associated with the inviscid instability of the jet mean flow shear layer. These instabilities in turn generate sound which provides the primary loading for the panels. The resulting structural vibration and radiation depends strongly on their placement relative to the jet/nozzle configuration. Results are obtained for the panel responses as well as the transmitted and incident pressure. The effect of the panels is to act as a narrow filter, converting the relatively broad band forcing, heavily influenced by jet instabilities, into radiation concentrated in narrow spectral bands.

14. SUBJECT TERMS	15. NUMBER OF PAGES
Jet noise, radiation, structure	29
	16. PRICE CODE: A03

17. SECURITY CLASSIFICATION OF REPORT	18. SECURITY CLASSIFICATION OF THIS PAGE	19. SECURITY CLASSIFICATION OF ABSTRACT	20. LIMITATION OF ABSTRACT
Unclassified	Unclassified		

NSN 7540-01-280-5500

Standard Form 298(Rev. 2-89)
Prescribed by ANSI Std. Z39-18
298-102

☆U.S. GOVERNMENT PRINTING OFFICE 1994—528-064/23,033